9-28-2021

Periodically Disturbing the Spatial Structure of Biofilms Can Affect the Production of an Essential Virulence Factor in Pseudomonas aeruginosa

Rebecca J. Quinn
Nova Southeastern University

Ivana Barraza
Nova Southeastern University

Laura García-Diéguez
Nova Southeastern University

Camryn Pajon
Nova Southeastern University

Lauren E. Krausfeldt
Nova Southeastern University

AMERICAN SOCIETY FOR MICROBIOLOGY | mSystems®

RESEARCH ARTICLE

Periodically Disturbing the Spatial Structure of Biofilms Can Affect the Production of an Essential Virulence Factor in *Pseudomonas aeruginosa*

Rebecca J. Quinn,[a] Ivana Barraza,[a] Laura García-Diéguez,[a] Camryn Pajon,[a] Lauren E. Krausfeldt,[a] Kerollos Ibrahim,[a] Laura A. Enzinna,[a] Morgan E. Thorn,[a] Omar Tonsi Eldakar,[a] Travis J. A. Craddock,[b,c,d,e] Robert P. Smith[a]

[a]Department of Biological Sciences, Halmos College of Arts and Science, Nova Southeastern University, Fort Lauderdale, Florida, USA
[b]Clinical Systems Biology Group, Institute for Neuro-Immune Medicine, Nova Southeastern University, Fort Lauderdale, Florida, USA
[c]Department of Psychology and Neuroscience, College of Psychology, Nova Southeastern University, Fort Lauderdale, Florida, USA
[d]Department of Computer Science, College of Engineering and Computing, Nova Southeastern University, Fort Lauderdale, Florida, USA
[e]Department of Clinical Immunology, College of Osteopathic Medicine, Nova Southeastern University, Fort Lauderdale, Florida, USA

ABSTRACT Understanding the environmental factors that affect the production of virulence factors has major implications in evolution and medicine. While spatial structure is important in virulence factor production, observations of this relationship have occurred in undisturbed or continuously disturbed environments. However, natural environments are subject to periodic fluctuations, including changes in physical forces, which could alter the spatial structure of bacterial populations and impact virulence factor production. Using *Pseudomonas aeruginosa* PA14, we periodically applied a physical force to biofilms and examined production of pyoverdine. Intermediate frequencies of disturbance reduced the amount of pyoverdine produced compared to undisturbed or frequently disturbed conditions. To explore the generality of this finding, we examined how an intermediate disturbance frequency affected pyoverdine production in 21 different strains of *P. aeruginosa*. Periodic disturbance increased, decreased, or did not change the amount of pyoverdine produced relative to undisturbed populations. Mathematical modeling predicts that interactions between pyoverdine synthesis rate and biofilm density determine the amount of pyoverdine synthesized. When the pyoverdine synthesis rates are high, depletion of the biofilm due to disturbance reduces the accumulation of pyoverdine. At intermediate synthesis rates, production of pyoverdine increases during disturbance as bacteria dispersed into the planktonic state enjoy increased growth and pyoverdine production rates. At low synthesis rates, disturbance does not alter the amount of pyoverdine produced since disturbance-driven access to nutrients does not augment pyoverdine synthesis. Our results suggest that environmental conditions shape robustness in the production of virulence factors and may lead to novel approaches to treat infections.

IMPORTANCE Virulence factors are required to cause infections. Previous work has shown that the spatial organization of a population, such as a biofilm, can increase the production of some virulence factors, including pyoverdine, which is produced by *Pseudomonas aeruginosa*. Pyoverdine is essential for the infection process, and reducing its production can limit infections. We have discovered that periodically changing the spatial structure of a biofilm of *P. aeruginosa* strain PA14 using a physical force can reduce the production of pyoverdine. A mathematical model suggests that this is due to the disruption of spatial organization. Using additional strains of *P. aeruginosa* isolated from patients and the environment, we use experiments and modeling to show that this reduction in pyoverdine is due to interactions between biofilm density and the synthesis rate of pyoverdine. Our results identify conditions where pyoverdine production is reduced and may lead to novel ways to treat infections.

Citation Quinn RJ, Barraza I, García-Diéguez L, Pajon C, Krausfeldt LE, Ibrahim K, Enzinna LA, Thorn ME, Eldakar OT, Craddock TJA, Smith RP. 2021. Periodically disturbing the spatial structure of biofilms can affect the production of an essential virulence factor in *Pseudomonas aeruginosa*. mSystems 6:e00961-21. https://doi.org/10.1128/mSystems.00961-21.

Editor Yogendra Singh, University of Delhi

Address correspondence to Robert P. Smith, rsmith@nova.edu.

Received 26 July 2021
Accepted 7 September 2021
Published 28 September 2021

KEYWORDS *Pseudomonas aeruginosa*, pyoverdine, biofilms, disturbance, mathematical modeling, virulence factors

Virulence factors enable bacteria to colonize hosts, cause disease, and interfere with immune systems (1). They are critical components of pathogenesis since their removal via genetic means can prevent infection (2). While the genetic underpinnings of virulence factor expression have been identified for numerous pathogens (3), less is known about how fluctuations in the growth environment affect the production of virulence factors. This is critical to understand; pathogens sense, respond, and adapt to the host growth environment (4, 5), and fluctuations can provide advantages to either the host or the pathogen (6). Understanding how fluctuations in the environment affect the production of virulence factors has implications in microbial ecology (7), evolution (8, 9), and medicine (10).

The spatial structure of a bacterial population is a key determinant of virulence factor production (11). The formation of spatially organized populations (e.g., biofilms) can lead to the enhanced production of virulence factors (see Table S1). For example, small diffusible molecules, such as those involved in quorum sensing, can accumulate inside biofilms, which can augment expression of downstream elements, including virulence factors (12). Alternatively, some virulence factors show increased expression when bacteria are in the planktonic state where spatial structure is minimized (13). Our understanding of how spatial structure influences virulence factor production is largely based upon studies that are performed in constantly disturbed (e.g., well-mixed tubes) or stationary conditions (e.g., agar plates). These conditions do not necessarily mimic natural environments where environmental conditions will fluctuate. One type of fluctuation that is important in perturbing spatial structure are changes in physical forces (14, 15). Changes in fluid flow can be observed in aquatic environments (16), in medical devices (17), and in hosts (18). These can change or abolish biofilm structure (19, 20). Vibrations, frictional forces, and additional mechanical stressors can impact surface attachment and biofilm morphology (21, 22). In a natural environment, these forces are not continuous; they can fluctuate or occur periodically. Both soils (23) and tissues (24) can experience periodic changes in vibrational forces and aqueous environments can experience rapid changes in fluid flow, which affect shear forces (25). If a periodic change in force is sufficiently strong, it can lead to change in the spatial structure of a bacterial population, which may impact virulence factor production. While plausible, this relationship remains unstudied. Discovering how periodic fluctuations in physical forces affect virulence factor production can help determine evolutionary constraints that shape virulence factor production and how the robustness of such systems change across growth environments. This may lead to strategies to attenuate virulence factor production.

In this study, we used experimentation and mathematical modeling to determine how disturbing the spatial structure of biofilms composed of *Pseudomonas aeruginosa* with periodically applied physical forces alters the production of pyoverdine. We studied *P. aeruginosa* since it can cause infections in a variety of tissues (26–28). Environments where *P. aeruginosa* inhabits (soils [29], the trachea [18] and catheters [30]) are subjected to periodic fluctuations in physical forces. We studied the virulence factor pyoverdine since it has a well-described production pathway (31) and is essential for biofilm formation (32) and virulence (33). The degree of spatial structure of the population influences the amount of pyoverdine produced; aggregates of bacteria show increased pyoverdine synthesis (34), cell-cell contacts can limit pyoverdine diffusion (35), and bacteria in the planktonic state show augmented pyoverdine synthesis relative to their biofilm state counterparts (13, 36). Pyoverdine has a well-described role in pathogenesis; after being secreted from the cell, it sequesters iron from the environment and then returns the sequestered iron to the bacteria. This augments growth, the production of pyoverdine, and the expression of additional virulence factors (31).

RESULTS

An experimental approach to disturbing the spatial structure of biofilms. To periodically disturb the spatial structure of biofilms using physical force, we used an

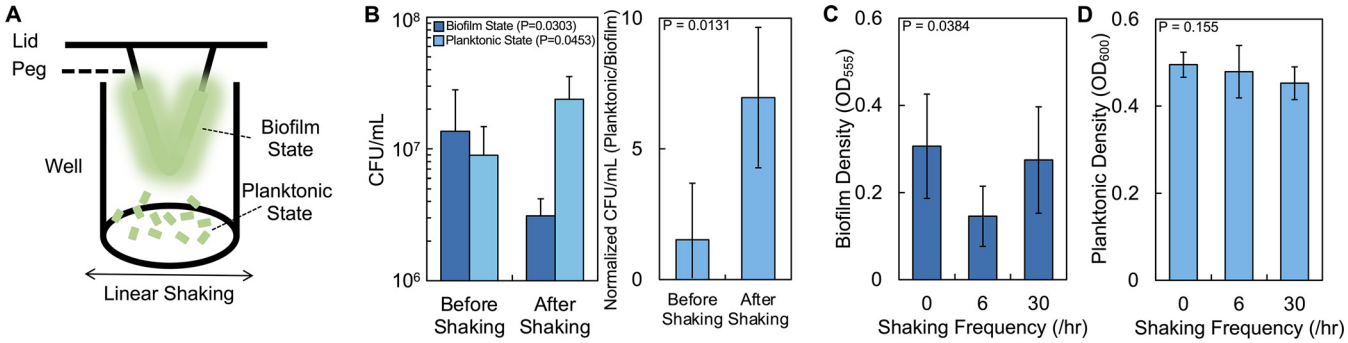

FIG 1 An experimental approach to periodically applying a physical force to structured bacterial populations. (A) We used the Innovotech MBEC Biofilm Inoculator device to grow biofilms. After growing biofilms, we used the linear shaking function of a plate reader to disturb the distribution of bacteria in the biofilm. (B) Density of bacteria in the biofilm and planktonic states before and after a single shaking event. (Left panel) Absolute cell density (biofilm, $P = 0.0303$, planktonic, $P = 0.0453$, Mann-Whitney [$P = 0.0006$, Shapiro-Wilk]). (Right panel) Planktonic cell density normalized by biofilm cell density ($P = 0.0131$, Mann-Whitney [$P = 0.0191$, Shapiro-Wilk]). Standard deviations from six biological replicates were determined. (C) Average biofilm density of strain PA14 at 24 h after shaking at the disturbance frequency indicated ($P = 0.0384$, one-way analysis of variance [ANOVA]). For panels C and D, standard deviations from a minimum of four biological replicates were determined. (D) Average density of bacteria in the planktonic state at 24 h after shaking at the disturbance frequency indicated ($P = 0.155$, one-way ANOVA).

MBEC biofilm inoculator device (Fig. 1A) (37). This system consists of a 96-well plate with rounded plastic pegs adhered to the inside of the lid. Each peg sits inside a well of a 96-well plate that contains liquid medium. Biofilms form on the peg, while bacteria in the planktonic state grow in the medium surrounding the peg. The density of bacteria in the biofilm and planktonic states can be measured using a crystal violet assay quantified at an optical density at 555 nm (OD_{555}) (38) and OD_{600}, respectively.

Our previous work demonstrated that we could use the linear shaking function of a microplate reader to perturb the spatial structure of bacteria embedded in soft agar (39). While the forces that *P. aeruginosa* can encounter in the environment are diverse, linear shaking captures the general effect of such forces: the ability to periodically alter the positions of bacteria. Physical forces encountered in natural environments, including changes in fluid flow (40) and additional mechanical forces (41), can transition bacteria between the biofilm and planktonic states. To determine whether we could use linear shaking to disrupt the spatial distribution of bacteria grown in the MBEC device, we grew biofilms composed of *P. aeruginosa* strain PA14 and quantified the density of bacteria in the biofilm and planktonic states before and after a single shaking event (Fig. 1B). We observed a significant increase in the density of bacteria in the planktonic state after a single shaking event, which coincided with a significant decrease in the density of bacteria in the biofilm state.

To determine how multiple shaking events over 24 h affected the distribution of bacteria in the biofilm and planktonic states, we grew biofilms of strain PA14 and subjected them to periodic shaking at three frequencies: 0 shakes/hour (0/h), 6/h, and 30/h. The 0/h and 30/h shakes served as the extremes of disturbance in our experiments; 0/h represented an undisturbed condition, and 30/h represented a frequently disturbed condition. 6/h served as an intermediate shaking frequency between these extremes. We observed a biphasic relationship between biofilm density and shaking frequency; biofilm density decreased at 6/h (relative to 0/h) but increased at 30/h (Fig. 1C). This increase at a high shaking frequency (30/h) is consistent with work showing that increasing shear force can promote biofilm formation (42, 43). In contrast, we observed a small, but insignificant, decrease in the density of bacteria in the planktonic state with increasing shaking frequency (Fig. 1D). Overall, using the linear shaking function of a plate reader could disrupt the spatial distribution of biofilms composed of *P. aeruginosa*.

Periodically disturbing the spatial structure of biofilms can alter the amount of pyoverdine. We next sought to examine how periodic disturbance would affect pyoverdine production. We grew biofilms of *P. aeruginosa* PA14 for 24 h, placed the biofilms in fresh medium and shook the biofilms at different frequencies. After 24 h, we quantified the amount of pyoverdine in the planktonic state and normalized this value by cell density (OD_{600}). At disturbance frequencies of 6/h, 12/h, and 20/h, there was a significant reduction in pyoverdine

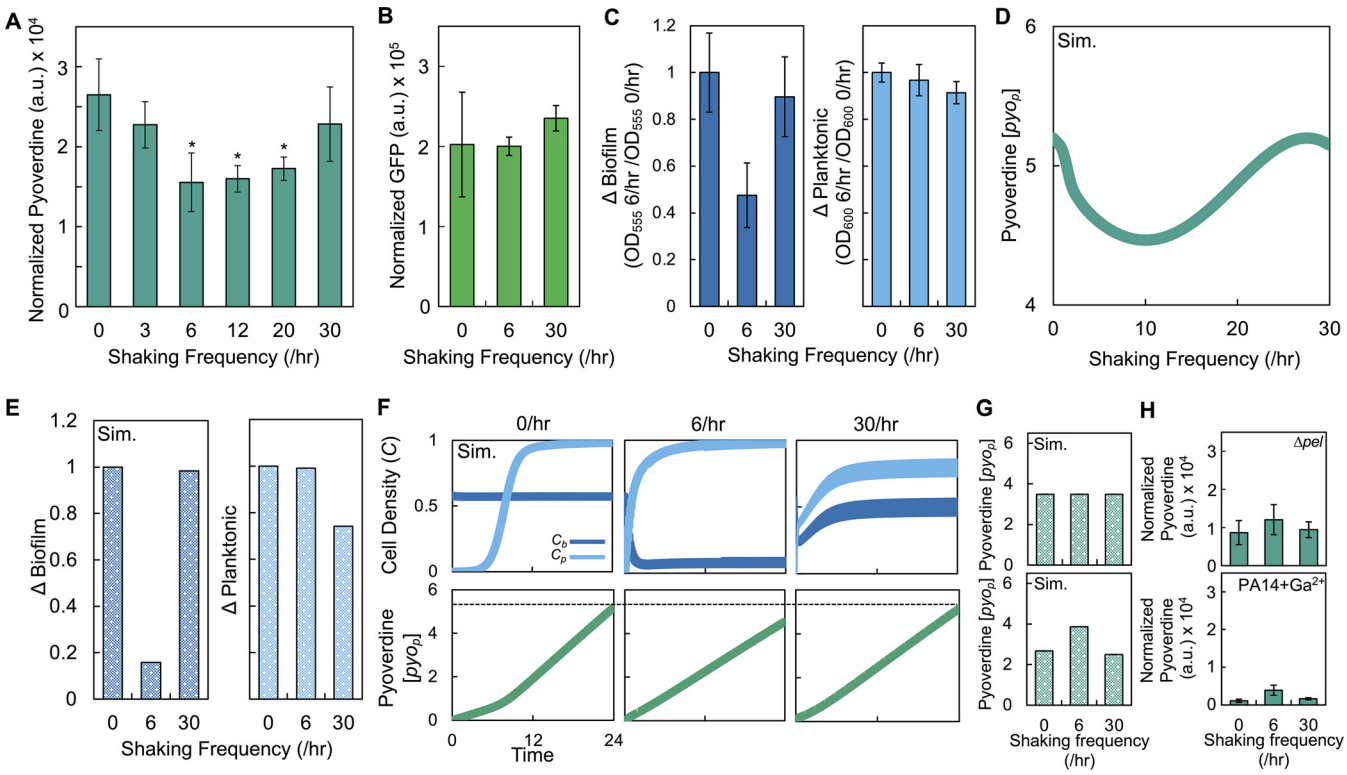

FIG 2 Periodically disturbing biofilms of *P. aeruginosa* strain PA14 can reduce the amount of pyoverdine. (A) Amount of pyoverdine in growth medium with 0% glucose after periodically disturbing biofilms composed of *P. aeruginosa* strain PA14 for 24 h. Pyoverdine normalized by cell density (OD_{600}). *, Significant differences between 0/h and 30/h ($P < 0.016$, two-tailed t test). For all panels, standard deviations from a minimum of three biological replicates were determined. The amount of pyoverdine is greater in the medium surrounding the peg compared to pyoverdine quantified from bacteria in the biofilm. Thus, we are measuring the majority of pyoverdine in our experiments (see Fig. S1A). We confirmed that we are measuring pyoverdine using a strain of PA14 that lacks the ability to make pyoverdine (Δ*pvd*; Fig. S1B) and a strain that lacks the ability to make pyocyanin (Δ*phz1* Δ*phz2*; Fig. S1C). (B) Amount of GFP produced by *P. aeruginosa* as a function of disturbance frequency. GFP (a.u.) was normalized by OD_{600}. There was a significant increase in GFP at 30/h relative to the 6/h condition ($P = 0.012$, two-tailed t test). Differences were not observed between 0/h and 6/h or 30/h ($P \geq 0.21$, two-tailed t test). (C) Change in the density of bacteria in the biofilm (Δbiofilm, left panel, $P = 0.0384$, one-way ANOVA) and planktonic (Δplanktonic, right panel, $P = 0.155$, one-way ANOVA) states due to periodic disturbance at 6/h and 30/h. (D) Simulations using equations 5 to 8 showing the effect of disturbance on pyoverdine synthesis. $t = 24$ h for panels D to G. The parameters are presented in Table S3. Sensitivity analysis results are shown in Fig. S1F. For panels D to G, Sim. = simulation results. (E) Simulated Δbiofilm and Δplanktonic values. (F) Simulations showing the temporal changes in the density of bacteria in the biofilm and planktonic states (top panels) and the amount of pyoverdine (bottom panels). The dotted line facilitates comparison between plots. (G) Simulations showing the effect of removing biofilm structure (top, C_b, $[pyo_b]$ and $[pyo_p] = 0$, $C_p = 0.1$) or reducing pyoverdine functionality (bottom, δ increased to 0.21 [from 0.11]). (H) Experiments showing the effect of removing biofilm structure (Δ*pel* strain, top, $P = 0.11$ [Kruskal-Wallis] and $P = 0.0011$ [Shapiro-Wilk]) or reducing pyoverdine functionality by adding 10 μM gallium to the medium (bottom, $P < 0.0001$ [Kruskal-Wallis] and $P < 0.0001$ [Shapiro-Wilk]).

relative to 0/h and 30/h (Fig. 2A). When biofilms composed of green fluorescent protein (GFP)-expressing *P. aeruginosa* were disturbed under the same conditions, GFP normalized by cell density (OD_{600}) did not show a decrease at 6/h (Fig. 2B). This indicated that the reduction of pyoverdine was not due to perturbations to gene expression.

To understand how periodic spatial disturbance over 24 h affected the distribution of bacteria compared to 0/h, we determined the relative change in the density of bacteria in the biofilm and planktonic states, which we call "Δbiofilm" and "Δplanktonic," respectively. To calculate Δbiofilm, we used crystal violet to measure the density of the biofilm after 24 h of disturbance. We then normalized each value by the density of the biofilm observed at 0/h. To calculate Δplanktonic, we used OD_{600} to measure the density of bacteria in the planktonic state after 24 h of disturbance. As described above, we normalized each value by the density of bacteria in the planktonic state observed at 0/h. We found that Δbiofilm was reduced at 6/h but remained relatively unchanged at 30/h compared to 0/h (Fig. 2C). Δplanktonic was insignificantly reduced at 30/h relative to 0/h, while at 6/h it was nearly indistinguishable from the 0/h value (Fig. 2C). This indicated that periodic disturbance reduced biofilm density at 6/h but had no significant influence on the density of bacteria in the planktonic state.

A reduction in biofilm density reduces pyoverdine synthesis at intermediate shaking frequency. One challenge with our experimental setup was the inability to measure the change in the distribution of bacteria and the amount of pyoverdine in real time or at multiple points during an experiment. This was owing to limitations of the MBEC device, where the peg serves to obscure the measurement of bacteria and pyoverdine without removing the lid. Removal of the lid during an experiment would alter the biofilm structure itself, which would confound our results. To overcome this challenge, we created a mathematical model that considers growth of bacteria and pyoverdine production of two distinct populations in the biofilm and planktonic states (see equations 5 to 8 in Materials and Methods). As in our experiments, we consider a population of bacteria in the biofilm state that have been placed in fresh medium (initially without bacteria in the planktonic state). Pyoverdine is synthesized by both populations according to first order kinetics and is dependent upon cell density. As previously observed (36), bacteria in the planktonic state have a higher pyoverdine synthesis rate relative to their biofilm state counterparts. However, as supported through RT-qPCR of *pvdA* (see Fig. S1 in the supplemental material), our model does not assume shaking frequency-dependent changes in the expression of genes involved in the synthesis of pyoverdine. That is, while bacteria in the planktonic state have increased pyoverdine synthesis owing to their positioning in the environment, this synthesis rate is consistent among all shaking frequencies. Bacteria grow in both states according to logistic growth that is scaled by the amount of pyoverdine in each state; increasing the amount of pyoverdine serves to increase the growth rate. This is consistent with previous work showing that removing pyoverdine synthesis through gene deletion (33) or attenuation of pyoverdine functionality (44) reduces the growth rate. In addition, bacteria in the planktonic state have a greater growth rate owing to additional nutrient access (45). Pyoverdine and bacteria in the biofilm state can diffuse to the planktonic state; the former was confirmed using a diffusion assay (see Fig. S1). Periodic disturbance transitions bacteria and pyoverdine into the planktonic state above the rate of diffusion. Bacteria can also transition from the planktonic state to the biofilm state in a shaking dependent fashion; as shaking increases, the amount of bacteria entering the biofilm state increases. This is consistent with studies that have demonstrated that increasing shear force promotes biofilm formation (42, 43). Model development and parameter estimation can be found in Materials and Methods. Parameters are presented in Table S3.

Our model predicts that the amount of pyoverdine is reduced at intermediate, but not high, shaking frequencies (Fig. 2D). Moreover, our model predicts the experimentally observed changes in Δbiofilm and Δplanktonic; Δbiofilm is reduced at 6/h, and Δplanktonic is reduced at 30/h (Fig. 2E). To understand the mechanism that led to a decrease in the amount of pyoverdine at 6/h, but not at 30/h, we simulated the temporal changes in the density of bacteria in the biofilm and planktonic states and the amount of pyoverdine (Fig. 2F). Our simulations predict that at 0/h, bacteria transition from the biofilm state into the planktonic state by diffusion, resulting in a high population density in both states after 24 h. The total amount of pyoverdine produced is a sum of pyoverdine synthesized by bacteria in biofilm state, which diffuses to the surrounding medium, and pyoverdine synthesized by bacteria in the planktonic state. At 6/h, the density of bacteria in the biofilm state is reduced owing to periodic disturbance. The rapid and sustained reduction in the density of bacteria in the biofilm state reduces the amount of pyoverdine that can diffuse from the biofilm into the surrounding medium. While there is an early increase in the number of bacteria in the planktonic state, the amount of pyoverdine produced by these bacteria is insufficient to compensate for the amount of pyoverdine lost due to the reduction in biofilm density. Accordingly, the total amount of pyoverdine produced by both populations is reduced compared to 0/h. At 30/h, frequent disturbance rapidly removes bacteria from the biofilm state into the planktonic state. However, as increased shear force promotes the formation of the biofilm, biofilm density is quickly restored. The combined effort of high-density populations in the biofilm, which contributes pyoverdine to the surrounding medium

via diffusion, and planktonic states synthesizes sufficient pyoverdine such that there is no difference between 0/h and 30/h.

Since our model predicts that the change in biofilm density is critical to changes in the amount of pyoverdine, we simulated the effect of removing biofilm structure. We initialized our simulations with a small population of bacteria in the planktonic state, without bacteria in the biofilm state, and removed the ability of the bacteria to transition from the planktonic state to the biofilm state. Our model predicts that the amount of pyoverdine during periodic disturbance does not change relative to 0/h (Fig. 2G, top). To test these predictions, we used a strain of *P. aeruginosa* that does not form biofilms (Δ*pel*) (46); periodic disturbance at 6/h and 30/h did not alter the amount of pyoverdine relative to 0/h (Fig. 2H, top). These results are consistent with our data (see Fig. S1) showing that the expression level of genes involved in pyoverdine synthesis do not change as a function of disturbance frequency. Otherwise, a reduction in the amount of pyoverdine at 6/h would have been observed. To examine how attenuating the functionality of pyoverdine would impact the effect of periodic disturbance on the amount of pyoverdine produced, we increased the value of δ in our model, which represents the maximal rate at which growth is reduced owing to lack of iron uptake via pyoverdine. Increasing δ would effectively decrease the functionality of pyoverdine; more pyoverdine would be required to augment growth relative to smaller values of δ. Our model predicts that the amount of pyoverdine increases at 6/h relative to 0/h and 30/h (Fig. 2G, bottom). To test this prediction, we disturbed biofilms of PA14 in the presence of gallium nitrate, which reduces pyoverdine functionality (44). We observed a significant increase in pyoverdine at 6/h, relative to 0/h and 30/h (Fig. 2H, bottom). This analysis provides support of our modeling predictions and shows that the presence of a biofilm and pyoverdine functionality are required to observe a decrease in pyoverdine at intermediate disturbance frequencies.

The reduction in pyoverdine at 6/h is consistent when biofilm density, pyoverdine synthesis, and growth rate are perturbed. Previous work has indicated that carbon sources can influence biofilm density, growth rate, and the amount of pyoverdine produced by pseudomonads (47–49). To determine how changes to these variables would affect the ability of disturbance to reduce pyoverdine at 6/h, we increased the percentage of glucose in the growth medium. This served to decrease biofilm density (Fig. 3A) and growth rate (Fig. 3B) but increased pyoverdine synthesis (Fig. 3C). The decrease in biofilm density with increasing glucose differs from a previous study that indicated glucose increases biofilm density (49). Quantification of biofilm density in the absence of the MBEC device confirmed these previous results (see Fig. S2). Next, we periodically disturbed biofilms formed in media with increasing glucose. We observed that the amount of pyoverdine decreased at 6/h (relative to 0/h and 30/h) when the percentage of glucose in the medium was increased. Quantification of Δbiofilm and Δplanktonic showed similar results to when 0% glucose was used in the medium; Δbiofilm showed a biphasic relationship with shaking frequency (Fig. 3D, left), whereas Δplanktonic was slightly reduced at 30/h (Fig. 3D, right). Our model predictions were consistent with these findings. To capture the effect of increasing the concentration of glucose in the medium, we simultaneously decreased growth rate and initial biofilm density, while increasing pyoverdine production rate (parameters in Table S3). Our model predicts a reduction in pyoverdine amount at 6/h (relative to 0/h and 30/h, Fig. 3E), that Δbiofilm is reduced at 6/h, and that Δplanktonic decreases at 30/h (Fig. 3F). Our combined experimental and modeling analysis show that the reduction in the amount of pyoverdine at 6/h is observable under conditions that alter initial biofilm density, growth rate, and pyoverdine synthesis rate.

Periodic disturbance can increase, decrease or leave the amount of pyoverdine unchanged. Environmental factors, such as pH and community diversity, can affect strain specific pyoverdine production rates (50). To examine how strains isolated from diverse environments would be impacted by periodic disturbance, we acquired 20 additional strains of *P. aeruginosa* that were isolated from the environment and the clinic (see Table S2). These strains varied in initial biofilm density, growth rate, and the amount of

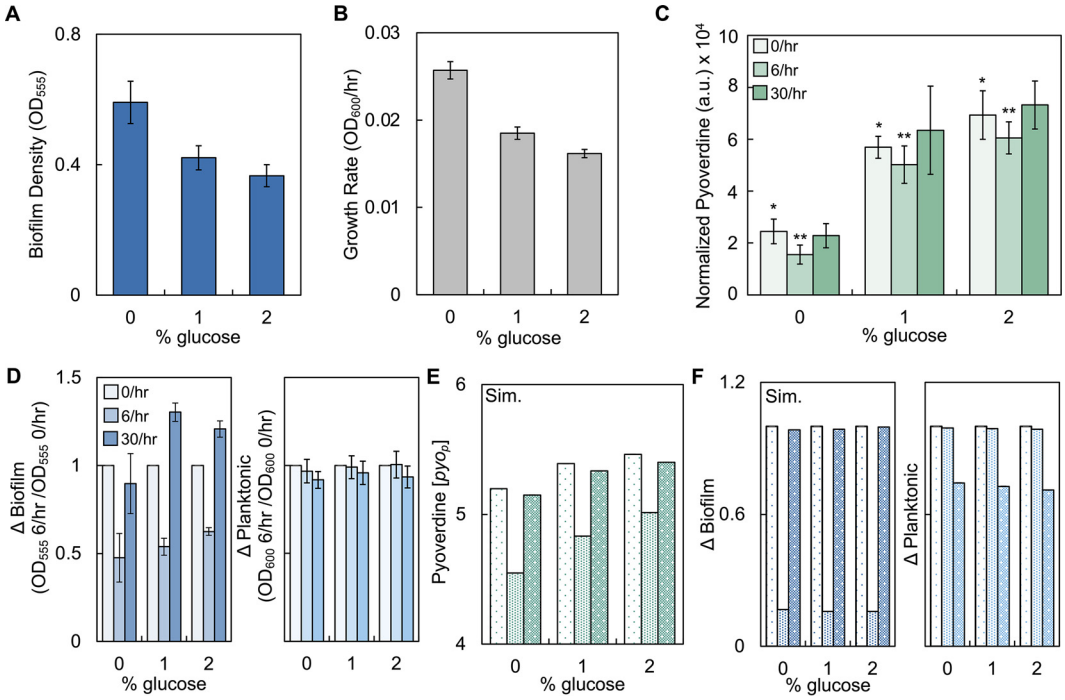

FIG 3 The decrease in pyoverdine is maintained when the initial biofilm density, growth rate, and pyoverdine synthesis are simultaneously perturbed using glucose. (A) Average initial biofilm density of *P. aeruginosa* grown in media with increasing percentages of glucose. $P < 0.0001$, one-way ANOVA. Standard deviations from five biological replicates were determined. (B) Average growth rate of *P. aeruginosa* in media with increasing glucose. $P < 0.001$, one-way ANOVA. Standard deviations from three biological replicates were determined. (C) Amount of pyoverdine in growth media with increasing percentages of glucose after periodically disturbing biofilms. Pyoverdine normalized by cell density (OD_{600}). *, Statistical difference between undisturbed condition across percentages of glucose ($P < 0.0001$, Kruskal-Wallis, Shapiro-Wilk, $P = 0.002$); **, statistical difference between undisturbed (0/h) and 30/h conditions ($P \leq 0.0317$, Mann-Whitney, all conditions, Shapiro-Wilk, $P < 0.0001$). (D) Change in the density of bacteria in biofilm (Δbiofilm, left panel, $P \leq 0.0384$ for all % glucose, one-way ANOVA) and planktonic (Δplanktonic, right panel, $P \geq 0.155$ for all % glucose, one-way ANOVA) states due to periodic disturbance at 6/h and 30/h. Standard deviations from a minimum of four biological replicates were determined. (E) Simulations showing the effect of changing growth rate (μ), initial biofilm density (C_b), and pyoverdine synthesis rate (k_s) on the amount of pyoverdine produced during periodic disturbance. For panels E and F, $t = 24$ h. Parameters are presented in Table S3. For all panels, Sim. = simulations results. (F) Simulated Δbiofilm and Δplanktonic values for the conditions depicted in panels E.

pyoverdine produced in the 0/h condition, but none of these characteristics were linearly correlated with each other (see Fig. S2). Thus, each strain represented a unique combination of growth rate, biofilm density, and pyoverdine synthesis. Using this set of strains, we could develop an understanding of the key facets of bacterial physiology that allowed pyoverdine to be reduced at 6/h. We chose to study 6/h since it resulted in the greatest reduction in pyoverdine synthesis in PA14 and was between the extreme conditions of disturbance (0/h and 30/h).

We grew biofilms of these strains in medium with 0, 1, and 2% glucose and disturbed each biofilm for 24 h at 6/h, whereupon we quantified the amount of pyoverdine. Our use of different growth media allowed us to study a large parameter space as including different percentages of glucose altered growth rate, biofilm density, and pyoverdine synthesis nonintuitively. For example, while increasing glucose decreased the growth rate for some strains, other strains showed an increase in growth rate, others had a biphasic relationship between growth rate and percentage of glucose in the medium (see Fig. S3). After 24 h of disturbance, we observed that strains showed an increase, decrease, or a lack of change in amount of pyoverdine produced at 6/h relative to 0/h as determined using a two-tailed *t* test (Fig. 4A). Thirty-seven strains/conditions tested did not result in a significant change in the amount of pyoverdine at 6/h (Fig. 4B), whereas 26 strains/conditions showed a significant difference in pyoverdine; 12 strains/conditions showed an increase, and 14 strains/conditions showed a decrease.

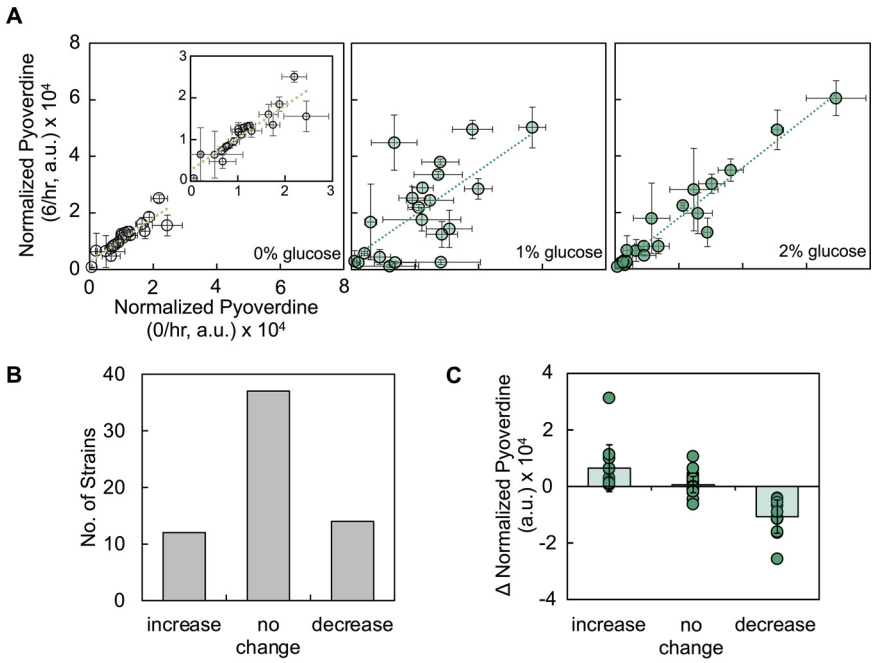

FIG 4 Strains of *P. aeruginosa* vary in their susceptibility to periodic disturbance at 6/h. (A) Amount of normalized pyoverdine produced by 21 different strains of *P. aeruginosa* in the undisturbed (0/h) and 6/h conditions when the growth media contained 0% (left, inset – reduced axes), 1% (center), and 2% (right) glucose. The amount of pyoverdine was normalized based on the cell density (OD_{600}). Standard deviations from a minimum of six biological replicates were determined. The line drawn serves as a guide; deviations from the line indicate differences in pyoverdine between the undisturbed and disturbed conditions. Raw data are provided in Fig. S5. (B) Number of strains that had an increase, no change, or a decrease in the amount of normalized pyoverdine produced at 6/h relative to 0/h. Significance was assessed using a two-tailed *t* test with a Benjamini-Hochberg correction to protect against false positives. (C) Change in normalized pyoverdine grouped by strains that had an increase, no change, or a decrease at 6/h compared to 0/h. $P < 0.0001$ using a Wilcoxon/Kruskal-Wallis test ($P < 0.0001$, Shapiro-Wilk test).

To determine why a disturbance at 6/h affected the amount of pyoverdine synthesized for some strains, but not others, we grouped the strains/conditions as follows based on their responses to disturbance: increase, decrease, and no change. The change in pyoverdine was significantly different across these groupings thus providing support for our grouping approach (Fig. 4C). To determine the impact of periodic disturbance on the distribution of bacteria, we quantified Δbiofilm and Δplanktonic. We observed a significant difference in Δbiofilm as a result of disturbance; Δbiofilm was smallest when a decrease in pyoverdine was observed and greatest when pyoverdine remained unchanged (Fig. 5A). A significant difference was not observed in Δplanktonic (Fig. 5A). Within each group, we quantified initial biofilm density, pyoverdine synthesis (0/h), final biofilm density (0/h), and growth rate. We found that there was a significant difference in pyoverdine synthesis between each group; pyoverdine synthesis was highest in the group that showed a decrease in the amount of pyoverdine, and it was the lowest in the group that did not show a change in pyoverdine amount (Fig. 5B). We did not find any significant differences in growth rate, initial biofilm density, motility, and final biofilm density at 0/h when strains were grouped based on their response to disturbance at 6/h (see Fig. S3). We also did not find a significant relationship between the combined effect of initial biofilm density and pyoverdine synthesis (0/h) on the change in pyoverdine owing to disturbance ($P = 0.1078$, multiple linear regression model, least-squares analysis). Finally, we did not find a consistent relationship between the effect of disturbance and the genetic diversity of strains or sequence diversity across proteins involved in pyoverdine synthesis (see Fig. S4). Overall, our analysis identified two key factors that were connected with a strain's response to disturbance at 6/h: differences in Δbiofilm and pyoverdine synthesis.

Next, we used our model to understand why disturbance at 6/h affected pyoverdine synthesis in some, but not all, strains. For these simulations, we varied the pyoverdine

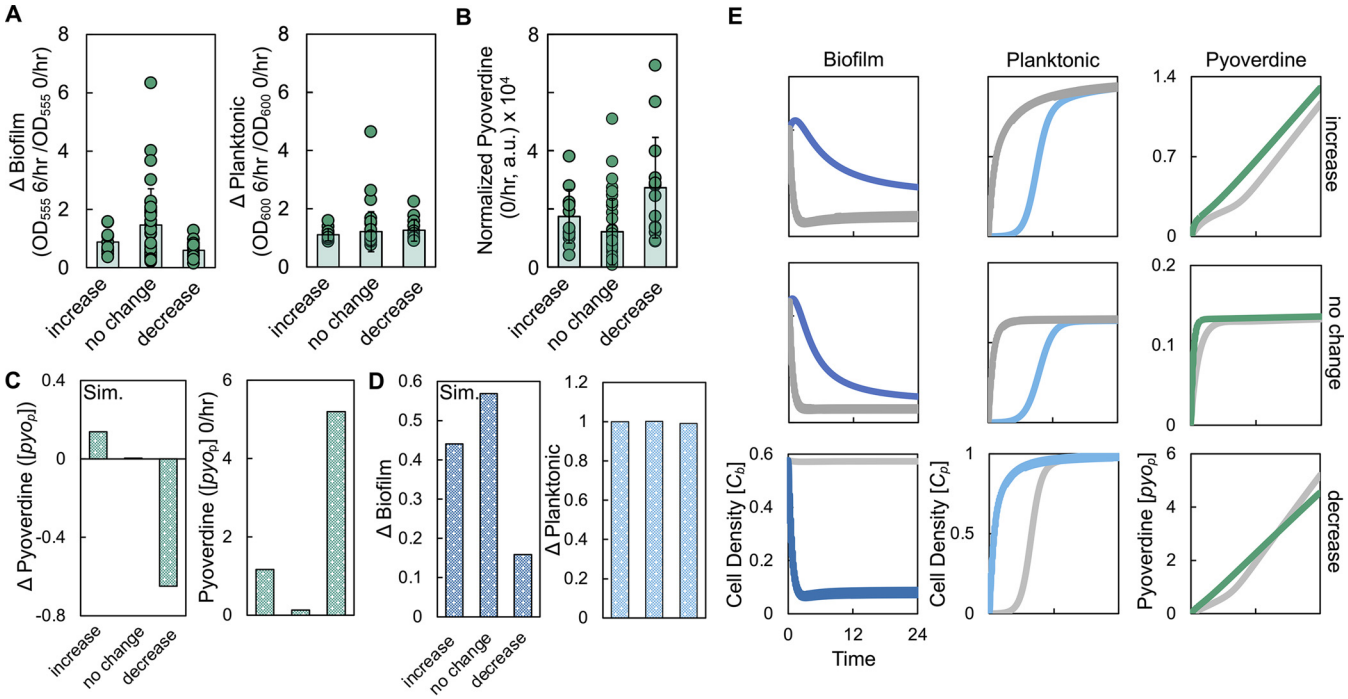

FIG 5 Changes in the density of the biofilm can account for the increase, decrease, or lack of change in the amount of pyoverdine as a result of periodic disturbance. (A) Experimental Δbiofilm (left panel, $P = 0.017$, Kruskal-Wallis) and Δplanktonic (right panel, $P = 0.2187$, Kruskal-Wallis, Shapiro-Wilk, $P < 0.0001$) values due to periodic disturbance at 6/h. Standard deviations from six biological replicates were determined. (B) Amounts of normalized pyoverdine produced in the 0/h condition grouped by strains that had an increase, no change, or a decrease at 6/h compared to 0/h ($P = 0.0011$, Kruskal-Wallis, Shapiro-Wilk, $P < 0.0001$). (C, left) Simulations showing the difference in pyoverdine between 0/h and 6/h for different pyoverdine synthesis rates. (C, right) Simulations showing the final amount of pyoverdine in the 0/h condition for different pyoverdine synthesis rates. For panels C to E, we used equations 5 to 8. Parameter values, including initial biofilm densities and pyoverdine synthesis rates, are provided in Table S3. $t = 24$ h. General trends in panels C to E can be found over longer simulation times (see Fig. S6B) and over a range of parameter values (see Fig. S7). For all panels, Sim. = simulation results. (D) Simulated Δbiofilm (left) and Δplanktonic (right) values. (E) Simulations showing the temporal changes in the density of bacteria in the biofilm (left) and planktonic states (center), as well as the amount of pyoverdine (right), for each pyoverdine synthesis rate.

synthesis rates (Fig. 5B) and the initial biofilm density (see Fig. S3) in accordance with our experimental results. With respect to the latter, our experimental results show that, on average, initial biofilm density is greatest in the decrease group and lowest in the increase group. Relaxing this assumption by making the initial biofilm density consistent across groupings does not change the qualitative features of our modeling predictions (see Fig. S6). Our simulations predict the general findings of our experiments (Fig. 5C and D). At a high pyoverdine synthesis rate, the total amount of pyoverdine produced is reduced at 6/h (compared to 0/h; Fig. 5C). This coincided with a small value of Δbiofilm and a value of Δplanktonic that was ~1 (Fig. 5D). A further reduction in pyoverdine synthesis rate served to increase the amount of pyoverdine produced in the 6/h condition (Fig. 5C). This coincided with an intermediate value of Δbiofilm and a value of Δplanktonic that was ~1 (Fig. 5D). Finally, a further reduction in pyoverdine synthesis rate resulted in a very small increase in the amount of pyoverdine produced at 6/h (Fig. 5C). This coincided with a large value of Δbiofilm and a value of Δplanktonic was ~1 (Fig. 5D). Overall, our simulations capture the trends of our experimental findings.

To understand the mechanism behind these findings, we simulated temporal changes in the density of bacteria in the biofilm and planktonic states, and the amount of pyoverdine under the 0/h and 6/h conditions. Our simulations predict that, in general, the density of bacteria in the biofilm state was reduced at 0/h owing to natural dispersal, which was consistent with our experimental findings (see Fig. S6). When pyoverdine synthesis is high and at 0/h, the amount of pyoverdine produced is high owing to a high density of bacteria in both the biofilm and planktonic states. Disturbance at 6/h reduces the density of the biofilm by transitioning bacteria into the planktonic

state at a rate greater than natural dispersal. Over 24 h, this does not result in a significant increase in the final density of bacteria in the planktonic state likely owing to the carrying capacity of the medium (Fig. 5D and E). While these bacteria have increased pyoverdine synthesis and growth owing to their position in the planktonic state, the reduction in pyoverdine synthesized by, and diffused from, bacteria in the reduced biofilm state cannot be compensated for by bacteria in the planktonic state. Thus, the overall amount of pyoverdine is reduced.

At an intermediate pyoverdine synthesis rate, the amount of pyoverdine produced by bacteria in the biofilm at 0/h is reduced owing to reductions in both pyoverdine synthesis rate and biofilm density. Disturbance at 6/h transitions bacteria from the biofilm into the planktonic state more rapidly than natural dispersal processes. This early and rapid increase in bacteria in the planktonic state serves to increase the total amount of pyoverdine synthesized as bacteria in this state as they take advantage of the higher pyoverdine synthesis and growth rates. When combined with the pyoverdine diffused from bacteria in the biofilm state, the overall amount of pyoverdine is increased.

Finally, at a low pyoverdine synthesis rate, the amount of pyoverdine produced by bacteria in the biofilm at 0/h is further reduced. As above, disturbance at 6/h transitions the bacteria into the planktonic state more quickly compared to natural dispersal. Although these bacteria produce pyoverdine at a higher synthesis rate, it is insufficient to lead to an appreciable increase in the total amount of pyoverdine synthesized. Thus, the total amount of pyoverdine synthesized remains largely unchanged between the undisturbed and 6/h conditions. These predictions are consistent when the values of parameters in our model, including the amount of pyoverdine and bacteria transitioned from the biofilm to the planktonic state owing to disturbance, are varied (see Fig. S7). Overall, interactions between pyoverdine synthesis rate and the relative change in biofilm density determines the effect that periodic disturbance has on the amount of pyoverdine produced by *P. aeruginosa* strains at 6/h.

DISCUSSION

We have shown that periodically disturbing the spatial structure of a biofilm of *P. aeruginosa* using a physical force can affect pyoverdine production. Our model suggests that changes in the amount of pyoverdine, or lack thereof, can be attributed to the change in the density of bacteria in the biofilm state owing to disturbance and the synthesis rate of pyoverdine. While we cannot rule out that additional factors may contribute to any changes in pyoverdine production, such as differences in oxygenation attributed to shaking, we did not find significant associations between initial biofilm density, biofilm density at 0/h, growth rate, diversity across the pyoverdine locus, or motility. It is likely that there is heterogeneity in pyoverdine expression in our system (35). However, this is unlikely to confound our results or mechanism as our model, which predicts the qualitative trends in our data over a wide parameter space (see Fig. S1 and S7), considers average population behavior only. Our analysis focused on a disturbance frequency of 6/h, which was driven by our initial observation that this frequency resulted in the greatest significant change in the quantity of pyoverdine produced from PA14 (Fig. 2). However, additional shaking frequencies, such as those greater or less than 6/h, may alter pyoverdine production differently for each strain. Moreover, the type of force applied to the biofilm may differentially affect pyoverdine production. While we used linear shaking to test the generality of fluctuations in physical force and their effect on the production of virulence factors, other types of physical forces will have additional considerations. For example, changes in flow rate would serve to remove secreted virulence factors from the system entirely, which may serve to further alter production. Thus, our experimental findings and model may not be relevant in all situations where periodic disturbances that affect spatial structure occur. Finally, while the molecular players involved in quorum sensing, such as the *Pseudomonas* quinolone signal (51), can influence pyoverdine production, production of pyoverdine is

largely regulated through non-quorum sensing means (31). Thus, although we cannot exclude the possibility that quorum sensing is influencing our findings, it likely plays a secondary role, which certainly warrants future exploration.

Previous work has noted differences in virulence factor expression, including pyoverdine, from strains isolated from the clinic and environment. Strains isolated from infections of various durations (52) and patients (53) show diversity in virulence factor expression. Differences in growth environments can lead to diverse selective pressures (54). Pressures unique to each strain might have shaped their ability to resist, or be altered by, periodic disturbance in terms of the amount of pyoverdine produced. For example, those strains where a reduction in pyoverdine was observed might have evolved in areas that are less prone to fluctuations in physical forces. Thus, they are ill adapted to such conditions, which results in a decrease in pyoverdine. Conversely, strains where changes in pyoverdine amount were not found might have evolved in areas that face frequent changes in physical force. Adapting to this type of environment would allow the strain to maintain a relatively constant amount of pyoverdine, which could facilitate the maintenance of virulence. While this is plausible, we did not find significant associations between isolation source (e.g., wound, urine, blood, etc.) and the effect of disturbance (not shown).

While our manuscript focused on the impact of disturbance to spatial structure, we also characterized the relationship between pyoverdine production and biofilm density across strains of *P. aeruginosa*. Previous work has found that biofilm formation can promote the production of pyoverdine but that this was not consistent for all strains (34). While our initial observation that increasing glucose concentration increased pyoverdine synthesis in strain PA14 was consistent with previous work performed in *Pseudomonas* sp. (48), this observation was not consistent for all strains (see Fig. S5). The relationship between pyoverdine synthesis and carbon source across strains is complex and may reflect a combination of carbon source preference (55), evolutionary constraints (50), and strain-specific genetic differences (56). In contrast to previous work (49), we did not observe that increasing the percentage of glucose in the medium increased biofilm density. However, this can likely be attributed to differences in methodology between our study and the previous study (49) in terms of growth medium (57), temperature (58), and forces under which biofilms were formed (59), all of which have been previously shown to impact biofilm density.

Disruption of virulence factor function (10), including pyoverdine (60, 61), has shown promise toward attenuating pathogenesis. However, these approaches place selective pressure directly on the virulence factor. Changes to spatial structure through the periodic application of physical force might spread the selection pressure out over multiple targets (e.g., genes involved in virulence factor production, biofilm formation, and/or quorum sensing). This could serve to limit evolution against such forces while reducing virulence factor production. Such an approach would require careful considerations; if disturbances increased the amount of virulence factor, this could further the infection process. Counterintuitively, disturbances may make the population more susceptible to antibiotics since there can be a negative correlation between antibiotic resistance and production of certain virulence factors (62). Conversely, if periodic disturbance decreased the amount of virulence factor, this could reduce infection severity and thus provide a novel mechanism to treat infections.

MATERIALS AND METHODS

Strains and growth conditions. *P. aeruginosa* strains used in this study are listed in Table S2. All experiments were performed in modified King's A medium (2% peptone [Fisher Scientific, Waltham, MA], 0.5% potassium sulfate, [Acros Organics, Fisher Scientific], 17 mM magnesium chloride [Alfa Aesar, Ward Hill, MA]) with different glucose concentrations (0, 1, or 2% glucose [VWR, Radnor, PA]). Single colonies of *P. aeruginosa* isolated from Luria-Bertani (LB) agar medium (MP Biomedicals, Solon, OH) were shaken overnight (250 rpm and 37°C) in 3 ml of liquid LB medium in culture tubes (Genesee Scientific, Morrisville, NC). Where applicable, gallium nitrate (Acros Organics) was added to the final concentration indicated. We used the Innovotech (Edmonton, Alberta, Canada) MBEC biofilm inoculator to grow biofilms (37). We grew overnight cultures of *P. aeruginosa*, washed the cells in fresh King's A medium, and

diluted them 1,000-fold into fresh modified King's A medium. We then placed 150 μl of culture into the wells of the plate and shook the plate at 110 rpm at 25°C for 24 h.

Dispersal of cells from biofilm. We grew biofilms in modified King's A medium. After 24 h of growth, we removed the plate and washed the pegs in 200 μl of fresh King's A medium to remove any unadhered cells. The washed biofilms were placed in 200 μl of fresh modified King's A medium, and the plate was placed in a Victor X4 plate reader preset to 25°C. The biofilms were then shaken once with an amplitude of 0.1 mm (fast setting, frequency = 4,800 mm/min, 10 s per shaking event, linear shaking feature which shakes the plate along the *x* axis). To measure the density of bacteria in the planktonic state, we removed 10 μl from the medium surrounding the peg. To measure the density of bacteria in the biofilm, the peg was removed from the lid of the MBEC plate using sterilized forceps. The peg was placed in 200 μl of fresh LB medium and vortexed the sample to remove bacteria. We counted the CFU in the King's A medium surrounding the plate by plating a serial dilution on LB agar.

Biofilm staining. We followed a previously published protocol (63). We grew biofilms as described above. After 24 h, we washed the pegs (which remained attached to the lid of the microplate) with 200 μl of fresh modified King's A medium for 10 s. The washed pegs were placed in 125 μl of 0.1% crystal violet (Acros Organics) for 10 min. We then washed the stained pegs in 200 μl of ddH_2O four times to remove excess crystal violet. Finally, we transferred the pegs to 200 μl of 30% acetic acid (Fisher Scientific) for 10 min to remove crystal violet from the biofilms. The amount of solubilized crystal violet was measured using OD_{555} in a Victor X4 plate reader (Perkin-Elmer, Waltham, MA). To measure biofilm density in the absence of MBEC plate, we followed the procedure outlined an a previous study (49). Single colonies of *P. aeruginosa* were grown in 3 ml of LB media for 24 h at 37°C and 250 rpm. Bacteria were diluted 200-fold into 200 μl of King's A media containing 0 and 2% glucose, respectively, in a 96-well microplate. The microplate was incubated at 37°C without shaking. After 24 h, bacteria in the planktonic state were carefully aspirated, and the biofilm adhered to the wells was washed three times with 1× phosphate buffer saline (PBS). Biofilms were stained with 200 μl of 0.25% (wt/vol) crystal violet solution for 15 min at room temperature, washed three times with PBS, and allowed to dry for 20 min. Then, 200 μl of 95% ethanol was added to the wells, followed by incubation at room temperature for 20 min. The absorbance was measured at 555 nm using a Victor X4 plate reader.

Periodic disturbance experiments. We grew biofilms in modified King's A medium. After 24 h, we removed the plate and washed the pegs in 200 μl of fresh King's A medium to remove any unadhered cells. The washed biofilms were placed in 200 μl of fresh modified King's A medium, and the plate was placed in a Victor X4 plate reader preset to 25°C. The plate was then periodically shaken (fast setting, frequency = 4,800 mm/min, 10 s per shaking event, linear shaking feature which shakes the plate along the *x* axis, amplitude = 0.1 mm) at the frequency indicated. After 24 h of growth in the plate reader, we removed the lid from the plate and measured the cell density (OD_{600}) and the concentration of pyoverdine using the Victor X4 microplate reader. Pyoverdine (arbitrary units) normalized by OD_{600}.

Measuring expression of GFP. We prepared competent *P. aeruginosa* PA14 as described previously (64). We transformed these cells with plasmid pAB1 (confers ampicillin resistance [65]), which contains an IPTG (isopropyl-β-D-thiogalactopyranoside)-inducible copy of enhanced GFP (eGFP). We grew biofilms of these GFP-expressing bacteria as described above under "Strains and growth conditions." After washing the pegs to remove any unadhered cells, we placed the biofilms into fresh modified King's A medium that contained, or did not contain as a control, 1 mM IPTG (Thermo Fisher). We then shook the biofilms periodically (or not at all as a control, 0/h) as described under "Periodic disturbance experiments" above. After 24 h, we quantified OD_{600} and GFP (λ_{excite}, 485 nm; $\lambda_{emission}$, 510 nm) using a Victor X4 microplate reader. GFP was normalized by OD_{600}.

RNA extraction and cDNA synthesis. To isolate total RNA, the Qiagen RNeasy minikit was used following the RNAprotect bacterial reagent handbook, with modifications. *P. aeruginosa* biofilms were grown as described above. From the MBEC plate, ~180 μl of medium was collected from each well and placed into 1.5-ml centrifuge tubes. Collected medium was then centrifuged for 2 min at 12,000 rpm. Pelleted cells were resuspended in 200 μl of RNase free water. Each tube was then centrifuged again for 2 min at 12,000 rpm. The remaining supernatant was discarded. After centrifugation, 30 μl of a 10 mg/ml solution of lysozyme (MP Biomedicals) in 1× Tris-EDTA (Thermo Fisher) was added to each centrifuge tube, followed by incubation at room temperature for 20 min with vortexing every 2 min. The total RNA was then extracted according to the manufacturer's recommended protocol, including the optional in-column DNase digestion using the RNase-Free DNase set. After RNA extraction, we used a Qiagen DNase Max kit according to the Quick Start protocol provided by the manufacturer. cDNA synthesis was performed using Bio-Rad reverse transcription supermix according to the manufacturer's recommendations in a Bio-Rad C1000 touch thermal cycler.

RT-qPCR. Quantitative real-time PCR was performed using the Bio-Rad iTaq Universal SYBR green Supermix and using a Bio-Rad CFX96 touch real-time PCR detection system. Expression of *rpoD* was detected using the primers *rpoD* F (GGCGAAGAAGGAAATGGTC) and *rpoD* R (CAGGTGGCGTAGGTGGAGAA) (66) (Sigma-Aldrich, Darmstadt, Germany). Expression of *pvdA* was quantified using the primers *pvdA* F (GACTCAGGCAACTGCAAC) and *pvdA* R (TGTCCAGGAACAGCACTTC) (Sigma-Aldrich). The parameters for each RT-qPCR cycle used were as follows: 95°C for 3 min, 95°C for 10 s, 63°C for 30 s, 63°C for 31 s, and 63°C for 5 s. A total of 40 cycles, followed by melting-curve analysis, were performed. Amplicon specificity and size were confirmed using agarose gel electrophoresis. The average threshold cycle (C_q) was normalized using the ΔC_T method (67). All C_T values were normalized using *rpoD*.

Measuring diffusion of pyoverdine. Biofilms of strain PA14 were grown for 24 h in modified King's medium with 0 or 2% glucose at 110 rpm and 25°C. The following day, biofilms were washed in 200 μl of 1× PBS to remove any unadhered bacteria, which limited the amount of pyoverdine produced by

bacteria dispersed from the biofilm into the surrounding medium. To further limit any natural dispersal or bacterial growth, biofilms were placed in 1× PBS for 1 h. We then filtered the medium surrounding the biofilm using a 0.45-μm filter (Genesee Scientific) to remove any dispersed bacteria and quantified pyoverdine in the cell-free medium. Pyoverdine values were blanked using background fluorescence produced from 1× PBS.

Growth rate. We determined the basal growth rate of the *P. aeruginosa* strains in the absence of biofilm formation. We grew each strain separately overnight in LB medium. The following day, each strain was diluted 200-fold into 200 μl of fresh modified King's A medium inside a 96-well plate. The plate was shaken at 250 rpm and at 25°C until the bacteria reached exponential phase (~4 h). We then measured the OD_{600} at regular intervals. We plotted a linear line through a plot of the OD_{600} versus time in h. The growth rate was determined using the slope of a linear line.

Dispersal rate. Single colonies were grown overnight in 3 ml of LB medium. The following day, 1 μl of bacteria was placed in the center of 5 ml of modified King's medium containing different percentages of glucose in the wells of a 6-well plate. Cultures were incubated for 24 h at 25°C. The radius from the center of the colony was measured using a ruler in three representative locations and was subsequently averaged for each replicate. The growth rate was determined from three biological replicates.

Phylogenetic analysis. Currently available draft genome assemblies were downloaded from the National Center for Biotechnology Information. Nucleotide sequences for 16S rRNA were aligned using MUSCLE (68), followed by phylogenetic analysis in MegaX v10.1.8. A maximum-likelihood tree was generated using the general time reversible model after 100 bootstrap iterations. Phylogenetic analysis was also performed using 49 concatenated single copy core genes from all *P. aeruginosa* draft genomes in KBase (69) using the application "Insert GenomeSet into Species Tree," which employs FastTree2 (70). To find genes in the synthesis of pyoverdine, open reading frames and annotations were performed with RAST (71). Amino acid sequences for each protein were either concatenated or analyzed alone by aligning with MUSCLE and generating a maximum-likelihood tree using the LG model after 100 bootstraps. Protein sequences for *pvd* genes that were detectable in 15 of 16 of the strains were used for concatenation. Proteins PvdT, PvdS, PvdL, PvdE, and PvdP were analyzed separately because they represented key steps in the pyoverdine process.

Statistical analysis. Statistical analysis as indicated in the text or figure legend. Unpaired *t* tests (unequal variance) were performed using Microsoft Excel (Redmond, WA). A Shapiro-Wilk test was used to assess normality. When evaluating the significance of changes in pyoverdine amount for strains grown in different media, we applied a Benjamini-Hochberg correction with a false discovery rate of 0.15. Additional tests were performed in JMP Pro 14 (SAS Institute, Inc., Cary, NC).

Model development and assumptions. We used the general modeling framework presented in earlier studies (72, 73) as the basis to develop our model. We used four ordinary differential equations, which included the production and decay of pyoverdine (equations 1 and 3) and growth of bacteria (equations 2 and 4).

$$\frac{d[pyo_b]}{dt} = -\beta[pyo_b] + k_{sb}C_b - k_d[pyo_b] \tag{1}$$

$$\frac{dC_b}{dt} = -\gamma C_b + \mu_b C_b\left(1 - \frac{C}{C_{\max}}\right) - \frac{\delta}{A + [pyo_b]}C_b \tag{2}$$

$$\frac{d[pyo_p]}{dt} = -\beta[pyo_b] + k_{sp}C_p - k_d[pyo_p] \tag{3}$$

$$\frac{dC_p}{dt} = \gamma C_b + \mu_p C_p\left(1 - \frac{C}{C_{\max}}\right) - \frac{\delta}{A + [pyo_b]}C_p \tag{4}$$

In these equations and in equations 5 to 8 below, subscripts *b* and *p* represent parameters that are associated with bacteria in the biofilm and planktonic states, respectively. *C* represents cell density, C_{max} represents the carrying capacity, k_s (μM/h) represents the synthesis rate constant of pyoverdine, "[*pyo*]" (μM) represents the concentration of pyoverdine, k_d (/h) represents the degradation rate of pyoverdine, μ represents growth rate (/h), γ represents the fraction of bacteria moving from the biofilm to the planktonic state owing to natural processes, β represents the fraction of pyoverdine that diffuses from the biofilm to the planktonic state, δ (μM/h) represents the maximal rate at which growth is reduced owing to lack of iron uptake via pyoverdine, A (μM) represents the concentration of pyoverdine that leads to half maximal growth reduction, α is the frequency at which an amount of bacteria and pyoverdine, ε is transferred from the biofilm state into the planktonic state, σ is the fraction of bacteria that are recruited to the biofilm, and t represents time (h). Simulations were performed in MATLAB (R2020b; MathWorks, Inc., Natick, MA) using ode23s (t = 24 h). Additional parameters may be found in Table S3 in the supplemental material.

To develop our model, we consider two populations of bacteria: one population in the biofilm state (C_b) and one population in the planktonic state (C_p). Both populations grow according to logistic growth at a growth rate of μ_b and μ_p, respectively. Each population has its own carrying capacity, C_{max}, which is normalized to 1. Thus, total cell density is always scaled to a maximum of 1. Populations in the biofilm and planktonic states produce pyoverdine according to first-order kinetics at a rate of k_{sb} and k_{sp}, respectively. Pyoverdine production is dependent upon the density of bacteria in each state. For simplicity, we

assume that pyoverdine degrades according to first-order kinetics at a rate of k_d, the value of which is consistent for both populations (74). Pyoverdine produced by the bacteria in the biofilm state diffuses into the surrounding medium at a rate of β. Bacteria from the biofilm state can move to the planktonic state at a rate of γ to account for natural dispersal, diffusion, and sloughing (75).

Consistent with previous studies that have examined the biosynthesis and utilization of pyoverdine (76, 77), we modeled the impact of pyoverdine on cell growth as a modified Michaelis-Menten type equation. δ represents the maximal rate at which growth is reduced owing to lack of iron uptake via pyoverdine, while A represents the concentration of pyoverdine that leads to half-maximal growth. The modified Michaelis-Menten term in our equations accounts for the observation that reducing pyoverdine functionality (44) or by removing the ability of *P. aeruginosa* to synthesize pyoverdine via gene deletion (78) reduces growth and biomass accumulation. As pyoverdine accumulates in the medium, any trace iron will be sequestered, which will facilitate growth. Thus, in the extreme case where pyoverdine is minimally produced, or not produced at all, growth is reduced. This is consistent with our data and previous literature (44, 79) showing that inhibiting pyoverdine functionality through deletion (see Fig. S1B) or the introduction of gallium (Fig. 2H) significantly reduces growth. However, as the concentration of pyoverdine reaches its maximum in the growth environment, growth will occur at the fastest possible rate (as dictated by μ in the logistic term). We note that while a sufficiently high concentration of iron can attenuate pyoverdine production (31), we did not explicitly model this interaction as we grew the bacteria in an iron limited environment and thus this could not be reached in our system.

Simulating the effect of periodic disturbance. To simulate the effect of periodic disturbance, we take a similar approach to previous work (72). At a given frequency (α), an amount of bacteria and pyoverdine (ε) is transferred from the biofilm state into the planktonic state. Thus, we modify equations 1 to 4 as follows:

$$\frac{d[pyo_b]}{dt} = -\varepsilon[pyo_b]\alpha(t_1) - \beta[pyo_b] + k_{sb}C_b - k_d[pyo_b] \tag{5}$$

$$\frac{dC_b}{dt} = \sigma C_p - \varepsilon C_b\alpha(t_1) - \gamma C_b + \mu_b C_b + \mu_b C_b\left(1 - \frac{C}{C_{\max}}\right) - \frac{\delta}{A + [pyo_b]}C_b \tag{6}$$

$$\frac{d[pyo_p]}{dt} = \varepsilon[pyo_b]\alpha(t_1) + \beta[pyo_b] + k_{sp}C_p - k_d[pyo_p] \tag{7}$$

$$\frac{dC_p}{dt} = -\sigma C_p + \varepsilon C_b\alpha(t_1) + \gamma C_b + \mu_p C_p\left(1 - \frac{C}{C_{\max}}\right) - \frac{\delta}{A + [pyo_b]}C_p \tag{8}$$

where $\alpha(t_1)$ is a dirac delta function where $t_1 = kT_0$, and T_0 represents the frequency of transfer events. ε accounts for the movement of both bacteria and pyoverdine so that any pyoverdine that is sequestered by the bacteria (e.g., through cell-cell contacts in the biofilm) at the moment of movement owing to periodic disturbance is transferred into the planktonic state, and σ represents the shaking dependent transfer of bacteria from the planktonic state back to the biofilm state. We included the σ term to account for previous studies that have shown that increased shear force causes recruitment of bacteria from the planktonic state back to the biofilm state (42, 43).

Parameter estimation. Parameters used in our mathematical model can be found in Table S3. We estimated the maximum growth rate of bacteria in the planktonic state (μ_p) from previously published work (80). Previous studies have demonstrated that spatial organization (81, 82), including biofilms (45, 83), can reduce access to nutrients to cells on the inside of spatial structures, including biofilms. In contrast, bacteria in the planktonic state have greater access to nutrients as they will not be surrounded by as many competitors compared to bacteria in the biofilm state. Accordingly, we assume that the growth rate of bacteria in the biofilm is less than the growth rate of bacteria in the planktonic state. Thus, we estimated that μ_b is reduced by 20% relative to μ_p to account for nutrient limitation in the biofilm (73).

Previous work has indicated that the average amount of pyoverdine synthesized by a colony of *P. aeruginosa* PAO1 is ~2 μM after 7 h of growth (35). Since our experiments occur over 24 h, we estimated that the total amount of pyoverdine synthesized would be approximately 5 to 8 μM. We therefore scaled the pyoverdine synthesis rate, k_{sb}, such that the final amount of pyoverdine produced by a population (both C_b and C_p combined) of strain PA14 was within this range of pyoverdine concentration. Note that our model and experimental measurements consider pyoverdine synthesis performed by a mature biofilm, and not pyoverdine production during the formation of a biofilm from a population initiated from the planktonic state.

Previous work has indicated that the rate of *pvdS* synthesis is increased ~5-fold in planktonic cells compared to cells in the biofilm (13). Increases in proteins involved in pyoverdine synthesis are also observed in planktonic bacteria (84). Moreover, aggregates from planktonic bacteria show increased pyoverdine amounts (2-fold) and *pvdS* expression (4-fold). However, other papers have indicated that biofilm formation is required for pyoverdine production (85). To account for these conflicting observations, we took an intermediate approach and adjusted the value of k_{sp} such that it is ~20% greater than k_{sb}. Relaxing this assumption, such that $k_{sp} = k_{sb}$ does not qualitatively affect our model predictions (see Fig. S1F).

The degradation rate of pyoverdine (k_d) was estimated using a previously published value that examined the dilution of pyoverdine (0.0085/min or ~0.5/h) in growing cells (86). While passive degradation

of pyoverdine is likely to occur in our system, most pyoverdine appears to be recycled (87). To account for the stability of pyoverdine, we reduced the order of magnitude of the degradation rate by 100-fold (~0.005/h).

To estimate the diffusion rate of pyoverdine, β, we considered that the vast majority, but not all, pyoverdine will immediately diffuse away from its production source. We assumed that not all pyoverdine would diffuse away from the biofilm as previous work has indicated that cell-cell contacts can augment the accumulation of pyoverdine, likely by limiting its diffusion (35). Thus, we estimated that 0.7 to 0.9 of pyoverdine from the biofilm will diffuse into the surrounding medium that contains bacteria in the planktonic state. We note that because of our experimental setup (grow biofilm for 24 h, wash in fresh medium, place biofilms in fresh medium, and begin shaking in the microplate reader), diffusion of pyoverdine from the biofilm to the planktonic state is the initial and predominant direction in which pyoverdine moves in our system.

Dispersal from a biofilm may be due to passive diffusion, sloughing, or active dispersal mechanisms (75). To estimate γ, we considered previously published data that showed that 1 to 10% of *Pseudomonas* disperse from mature biofilms (growth for 4 days) (88, 89) and occurs in response to nutrient stress/deprivation (90). However, because our biofilms are substantially younger (24 h) and we supply fresh medium just prior to shaking, we estimate that less than 1 to 10% of the population (when scaled to C_m, this would represent $C = 0.01$ to 0.1) will undergo dispersal over the 24-h period during which the plate is periodically perturbed. Finally, because we chose to grow the bacteria in an iron limited environment, iron driven biofilm dispersal likely does not occur. Indeed, such dispersal appears to commence occurring if 50 μM ferric sulfate is provided, which is substantially higher than any trace amount of iron or iron-complexed molecule that would be included in our system (91). Accordingly, we estimated that the dispersal rate of bacteria from the biofilm (C_b) to the planktonic state (C_p) will be approximately 0.001 to 0.0001/h (where C_{max} for C_b and $C_p = 1$). The values of δ and A were fit such that the total amount of pyoverdine produced by a population ($[pyo_b]+[pyo_p]$) of strain PA14 without periodic disturbance was approximately 5 to 6 μM over the total simulated time (24 h) (35).

ε was estimated using data presented in Fig. 1B showing the effect of a single shaking event on the number of bacteria dispersed from the biofilm (0.23 average decrease in biofilm density and 0.26 increase in planktonic density). Thus, we estimated that ε would lie within the approximate range of 0.1 to 0.3. σ was fit to a third order polynomial function such that the value of σ increased with increasing shaking frequency. We fit this value to a polynomial function (with the equation $\sigma = (3.95 \times 10^{-4})x^3 - (7.83 \times 10^{-3})x^2 + (5.39 \times 10^{-2})x - 4.84 \times 10^{-4}$, norm of residuals = 0.0011277) since previous work has shown a nonlinear increase in biofilm density with increasing shear force (42). We note, however, if the shear force is too high, biofilm density decreases. We do not appear to achieve this sufficiently high shear force in our system because at the highest shaking frequency tested (30/h), biofilm density is not significantly reduced compared to 0/h (Fig. 1C, Fig. 2C and Fig. 3D). Finally, α, which represents the frequency of transfer events, was matched to the experimental condition (6 shakes/h = transfer frequency of 1/6).

In accordance with our experimental protocol where a biofilm is formed prior to shaking, all simulations were initialized with 0.133 μM pyoverdine in the biofilm state and a population of bacteria in the biofilm state where $C_b = 0.577$ (where $C_{max} = 1$). Note that in our system, $C_b = C_{max}$ only when dispersal of bacteria due to natural processes does not occur. We used values of 0.133 μM and $C_b = 0.577$ since these values allowed a near-constant biofilm density to be maintained in the absence of shaking (Fig. 2F). However, as dictated by trends in our experimental data for strains other than PA14, the initial biofilm density was varied (see Table S3).

SUPPLEMENTAL MATERIAL

Supplemental material is available online only.

FIG S1, JPG file, 0.5 MB.
FIG S2, JPG file, 0.6 MB.
FIG S3, JPG file, 0.7 MB.
FIG S4, JPG file, 0.4 MB.
FIG S5, JPG file, 0.5 MB.
FIG S6, JPG file, 0.5 MB.
FIG S7, JPG file, 0.5 MB.
TABLE S1, DOCX file, 0.01 MB.
TABLE S2, DOCX file, 0.01 MB.
TABLE S3, DOCX file, 0.02 MB.

ACKNOWLEDGMENTS

Research was sponsored by the Army Research Office and was accomplished under grant W911NF-18-1-0443. The views and conclusions contained in this document are those of the authors and should not be interpreted as representing the official policies, either expressed or implied, of the Army Research Office or the U.S. Government. The U.S. Government is authorized to reproduce and distribute reprints for Government purposes notwithstanding any copyright notation here. The following reagents were

obtained through BEI Resources, NIAID, NIH: *Pseudomonas aeruginosa* strains MRSN 317, NR-5151, MRSN 512, NR-51518, MRSN 994, NR-51519, MRSN 1356, NR-51521, MRSN 1344, NR-51520, MRSN 1380, NR-51522, MRSN 1388, NR-51523, MRSN 1583, NR-57524, MRSN 1601, NR-51525, MRSN 16344, NR-51581, MRSN 16383, NR-51583, MRSN 16847, NR-51586, MRSN 17849, and NR-51587. These strains are part of the *Pseudomonas aeruginosa* Diversity Panel provided by the Multidrug-Resistant Organism Repository and Surveillance Network (MRSN) at the Walter Reed Army Institute of Research (WRAIR), Silver Spring, MD, USA. The following reagents were also obtained through BEI Resources, NIAID, NIH: *Pseudomonas aeruginosa* strains Shr42, NR-48982, EnvKY1, NR-51329, MX0560, NR-51334, Pa1400, NR-51335, Pa1651, NR-51336, PAK, NR-51337, Pa1414, and NR-51345.

We thank Roberto Kolter for his kind gift of the Δ*pel* strain, Natasha Kirienko for her kind gift of the Δ*pvd* strain, and Dianne Newman for her kind gift of the Δ*phz1* Δ*phz2* strain. We thank Cheemeng Tan for his help with preliminary coding for the mathematical model.

R.J.Q. and R.P.S. conceived and designed research. R.J.Q., I.B., L.G.-D., C.P., L.E.K., K.I., L.A.E., and M.E.T. performed experiments. T.J.A.C. and R.P.S. performed coding. R.P.S. performed simulations. R.J.Q., I.B., L.G.-D., O.T.E., and R.P.S. wrote the manuscript. All authors approve of the manuscript.

REFERENCES

1. Cross AS. 2008. What is a virulence factor? Crit Care 12:197–196. https://doi.org/10.1186/cc7127.
2. Falkow S. 1988. Molecular Koch's postulates applied to microbial pathogenicity. Rev Infect Dis 10(Suppl 2):S274–S276. https://doi.org/10.1093/cid/10.supplement_2.s274.
3. Winzer K, Williams P. 2001. Quorum sensing and the regulation of virulence gene expression in pathogenic bacteria. Int J Med Microbiol 291:131–143. https://doi.org/10.1078/1438-4221-00110.
4. Romani L, Bistoni F, Puccetti P. 2003. Adaptation of *Candida albicans* to the host environment: the role of morphogenesis in virulence and survival in mammalian hosts. Curr Opin Microbiol 6:338–343. https://doi.org/10.1016/s1369-5274(03)00081-x.
5. Do H, Makthal N, VanderWal AR, Saavedra MO, Olsen RJ, Musser JM, Kumaraswami M. 2019. Environmental pH and peptide signaling control virulence of *Streptococcus pyogenes* via a quorum-sensing pathway. Nat Commun 10:2586. https://doi.org/10.1038/s41467-019-10556-8.
6. Longo AV, Zamudio KR. 2017. Environmental fluctuations and host skin bacteria shift survival advantage between frogs and their fungal pathogen. ISME J 11:349–361. https://doi.org/10.1038/ismej.2016.138.
7. Harrison F. 2007. Microbial ecology of the cystic fibrosis lung. Microbiology (Reading) 153:917–923. https://doi.org/10.1099/mic.0.2006/004077-0.
8. Granato ET, Ziegenhain C, Marvig RL, Kümmerli R. 2018. Low spatial structure and selection against secreted virulence factors attenuates pathogenicity in *Pseudomonas aeruginosa*. ISME J 12:2907–2918. https://doi.org/10.1038/s41396-018-0231-9.
9. Montarry J, Hamelin FM, Glais I, Corbi R, Andrivon D. 2010. Fitness costs associated with unnecessary virulence factors and life history traits: evolutionary insights from the potato late blight pathogen *Phytophthora infestans*. BMC Evol Biol 10:283–289. https://doi.org/10.1186/1471-2148-10-283.
10. Heras B, Scanlon MJ, Martin JL. 2015. Targeting virulence not viability in the search for future antibacterials. Br J Clin Pharmacol 79:208–215. https://doi.org/10.1111/bcp.12356.
11. West SA, Buckling A. 2003. Cooperation, virulence, and siderophore production in bacterial parasites. Proc Biol Sci 270:37–44. https://doi.org/10.1098/rspb.2002.2209.
12. Darch SE, Simoska O, Fitzpatrick M, Barraza JP, Stevenson KJ, Bonnecaze RT, Shear JB, Whiteley M. 2018. Spatial determinants of quorum signaling in a *Pseudomonas aeruginosa* infection model. Proc Natl Acad Sci U S A 115:4779–4784. https://doi.org/10.1073/pnas.1719317115.
13. Chua SL, Liu Y, Yam JKH, Chen Y, Vejborg RM, Tan BGC, Kjelleberg S, Tolker-Nielsen T, Givskov M, Yang L. 2014. Dispersed cells represent a distinct stage in the transition from bacterial biofilm to planktonic lifestyles. Nat Commun 5:4462–4412. https://doi.org/10.1038/ncomms5462.
14. Persat A, Nadell CD, Kim MK, Ingremeau F, Siryaporn A, Drescher K, Wingreen NS, Bassler BL, Gitai Z, Stone HA. 2015. The mechanical world of bacteria. Cell 161:988–997. https://doi.org/10.1016/j.cell.2015.05.005.
15. Dufrêne YF, Persat A. 2020. Mechanomicrobiology: how bacteria sense and respond to forces. Nat Rev Microbiol 18:227–214. https://doi.org/10.1038/s41579-019-0314-2.
16. Droppo I, Krishnappan B, Liss S, Marvin C, Biberhofer J. 2011. Modeling sediment-microbial dynamics in the South Nation River, Ontario, Canada: towards the prediction of aquatic and human health risk. Water Res 45:3797–3809. https://doi.org/10.1016/j.watres.2011.04.032.
17. Donlan RM. 2001. Biofilms and device-associated infections. Emerg Infect Dis 7:277–281. https://doi.org/10.3201/eid0702.010226.
18. Hoegger MJ, Awadalla M, Namati E, Itani OA, Fischer AJ, Tucker AJ, Adam RJ, McLennan G, Hoffman EA, Stoltz DA, Welsh MJ. 2014. Assessing mucociliary transport of single particles *in vivo* shows variable speed and preference for the ventral trachea in newborn pigs. Proc Natl Acad Sci U S A 111:2355–2360. https://doi.org/10.1073/pnas.1323633111.
19. Purevdorj B, Costerton JW, Stoodley P. 2002. Influence of hydrodynamics and cell signaling on the structure and behavior of *Pseudomonas aeruginosa* biofilms. Appl Environ Microbiol 68:4457–4464. https://doi.org/10.1128/AEM.68.9.4457-4464.2002.
20. Rusconi R, Lecuyer S, Guglielmini L, Stone HA. 2010. Laminar flow around corners triggers the formation of biofilm streamers. J R Soc Interface 7:1293–1299. https://doi.org/10.1098/rsif.2010.0096.
21. Sjollema J, van der Mei HC, Hall CL, Peterson BW, de Vries J, Song L, de Jong ED, Busscher HJ, Swartjes JJ. 2017. Detachment and successive reattachment of multiple, reversibly-binding tethers result in irreversible bacterial adhesion to surfaces. Sci Rep 7:4369. https://doi.org/10.1038/s41598-017-04703-8.
22. Fei C, Mao S, Yan J, Alert R, Stone HA, Bassler BL, Wingreen NS, Košmrlj A. 2020. Nonuniform growth and surface friction determine bacterial biofilm morphology on soft substrates. Proc Natl Acad Sci U S A 117:7622–7632. https://doi.org/10.1073/pnas.1919607117.
23. Kim D-S, Lee J-S. 2000. Propagation and attenuation characteristics of various ground vibrations. Soil Dynamics Earthquake Eng 19:115–126. https://doi.org/10.1016/S0267-7261(00)00002-6.
24. Titze IR. 1976. On the mechanics of vocal-fold vibration. J Acoust Soc Am 60:1366–1380. https://doi.org/10.1121/1.381230.
25. Wheeler JD, Secchi E, Rusconi R, Stocker R. 2019. Not just going with the flow: the effects of fluid flow on bacteria and plankton. Annu Rev Cell Dev Biol 35:213–237. https://doi.org/10.1146/annurev-cellbio-100818-125119.
26. Barbier F, Andremont A, Wolff M, Bouadma L. 2013. Hospital-acquired pneumonia and ventilator-associated pneumonia: recent advances in epidemiology and management. Curr Opin Pulm Med 19:216–228. https://doi.org/10.1097/MCP.0b013e32835f27be.
27. Wagenlehner F, Naber K. 2000. Hospital-acquired urinary tract infections. J Hosp Infect 46:171–181. https://doi.org/10.1053/jhin.2000.0821.

28. Tredget EE, Shankowsky HA, Rennie R, Burrell RE, Logsetty S. 2004. *Pseudomonas* infections in the thermally injured patient. Burns 30:3–26. https://doi.org/10.1016/j.burns.2003.08.007.
29. Degens BP, Schipper LA, Sparling GP, Duncan LC. 2001. Is the microbial community in a soil with reduced catabolic diversity less resistant to stress or disturbance? Soil Biol Biochem 33:1143–1153. https://doi.org/10.1016/S0038-0717(01)00018-9.
30. Cole SJ, Records AR, Orr MW, Linden SB, Lee VT. 2014. Catheter-associated urinary tract infection by *Pseudomonas aeruginosa* is mediated by exopolysaccharide-independent biofilms. Infect Immun 82:2048–2058. https://doi.org/10.1128/IAI.01652-14.
31. Ringel MT, Brüser T. 2018. The biosynthesis of pyoverdines. Microb Cell 5:424–437. https://doi.org/10.15698/mic2018.10.649.
32. Banin E, Vasil ML, Greenberg EP. 2005. Iron and *Pseudomonas aeruginosa* biofilm formation. Proc Natl Acad Sci U S A 102:11076–11081. https://doi.org/10.1073/pnas.0504266102.
33. Meyer J-M, Neely A, Stintzi A, Georges C, Holder IA. 1996. Pyoverdin is essential for virulence of *Pseudomonas aeruginosa*. Infect Immun 64:518–523. https://doi.org/10.1128/iai.64.2.518-523.1996.
34. Kang D, Turner KE, Kirienko NV. 2017. PqsA promotes pyoverdine production via biofilm formation. Pathogens 7:3. https://doi.org/10.3390/pathogens7010003.
35. Julou T, Mora T, Guillon L, Croquette V, Schalk IJ, Bensimon D, Desprat N. 2013. Cell-cell contacts confine public goods diffusion inside *Pseudomonas aeruginosa* clonal microcolonies. Proc Natl Acad Sci U S A 110:12577–12582. https://doi.org/10.1073/pnas.1301428110.
36. Manos J, Arthur J, Rose B, Bell S, Tingpej P, Hu H, Webb J, Kjelleberg S, Gorrell MD, Bye P, Harbour C. 2009. Gene expression characteristics of a cystic fibrosis epidemic strain of *Pseudomonas aeruginosa* during biofilm and planktonic growth. FEMS Microbiol Lett 292:107–114. https://doi.org/10.1111/j.1574-6968.2008.01472.x.
37. Ceri H, Olson ME, Stremick C, Read RR, Morck D, Buret A. 1999. The Calgary Biofilm Device: new technology for rapid determination of antibiotic susceptibilities of bacterial biofilms. J Clin Microbiol 37:1771–1776. https://doi.org/10.1128/JCM.37.6.1771-1776.1999.
38. Haney EF, Trimble MJ, Cheng JT, Vallé Q, Hancock REW. 2018. Critical assessment of methods to quantify biofilm growth and evaluate antibiofilm activity of host defence peptides. Biomolecules 8:29. https://doi.org/10.3390/biom8020029.
39. Wilson CE, Lopatkin AJ, Craddock TJ, Driscoll WW, Eldakar OT, Lopez JV, Smith RP. 2017. Cooperation and competition shape ecological resistance during periodic spatial disturbance of engineered bacteria. Sci Rep 7:440. https://doi.org/10.1038/s41598-017-00588-9.
40. Ymele-Leki P, Ross JM. 2007. Erosion from *Staphylococcus aureus* biofilms grown under physiologically relevant fluid shear forces yields bacterial cells with reduced avidity to collagen. Appl Environ Microbiol 73:1834–1841. https://doi.org/10.1128/AEM.01319-06.
41. Ballance WC, Oh I, Lai Y, Elhebeary M, Saif T, Hu Y, Kong H. 2019. Vibration at structural resonance frequency of hydrophilic substrates enhances biofilm removal. Sensors Actuators B Chem 299:126950. https://doi.org/10.1016/j.snb.2019.126950.
42. Park A, Jeong H-H, Lee J, Kim KP, Lee C-S. 2011. Effect of shear stress on the formation of bacterial biofilm in a microfluidic channel. BioChip J 5:236–241. https://doi.org/10.1007/s13206-011-5307-9.
43. Yang J, Cheng S, Li C, Sun Y, Huang H. 2019. Shear stress affects biofilm structure and consequently current generation of bioanode in microbial electrochemical systems (MESS). Front Microbiol 10:398. https://doi.org/10.3389/fmicb.2019.00398.
44. Kaneko Y, Thoendel M, Olakanmi O, Britigan BE, Singh PK. 2007. The transition metal gallium disrupts *Pseudomonas aeruginosa* iron metabolism and has antimicrobial and antibiofilm activity. J Clin Invest 117:877–888. https://doi.org/10.1172/JCI30783.
45. Wentland EJ, Stewart PS, Huang CT, McFeters GA. 1996. Spatial variations in growth rate within *Klebsiella pneumoniae* colonies and biofilm. Biotechnol Prog 12:316–321. https://doi.org/10.1021/bp9600243.
46. Friedman L, Kolter R. 2003. Genes involved in matrix formation in *Pseudomonas aeruginosa* PA14 biofilms. Mol Microbiol 51:675–690. https://doi.org/10.1046/j.1365-2958.2003.03877.x.
47. Barbhaiya H, Rao K. 1985. Production of pyoverdine, the fluorescent pigment of *Pseudomonas aeruginosa* PAO1. FEMS Microbiol Lett 27:233–235. https://doi.org/10.1111/j.1574-6968.1985.tb00673.x.
48. Ponraj P, Shankar M, Ilakkiam D, Rajendhran J, Gunasekaran P. 2013. Influence of periplasmic oxidation of glucose on pyoverdine synthesis in *Pseudomonas putida* S11. Appl Microbiol Biotechnol 97:5027–5041. https://doi.org/10.1007/s00253-013-4737-9.
49. She P, Wang Y, Liu Y, Tan F, Chen L, Luo Z, Wu Y. 2019. Effects of exogenous glucose on *Pseudomonas aeruginosa* biofilm formation and antibiotic resistance. MicrobiologyOpen 8:e933. https://doi.org/10.1002/mbo3.933.
50. Butaitė E, Kramer J, Wyder S, Kümmerli R. 2018. Environmental determinants of pyoverdine production, exploitation and competition in natural *Pseudomonas* communities. Environ Microbiol 20:3629–3642. https://doi.org/10.1111/1462-2920.14355.
51. Popat R, Harrison F, Da Silva AC, Easton SA, McNally L, Williams P, Diggle SP. 2017. Environmental modification via a quorum sensing molecule influences the social landscape of siderophore production. Proc R Soc B Biol Sci 284:20170200. https://doi.org/10.1098/rspb.2017.0200.
52. Konings AF, Martin LW, Sharples KJ, Roddam LF, Latham R, Reid DW, Lamont IL. 2013. *Pseudomonas aeruginosa* uses multiple pathways to acquire iron during chronic infection in cystic fibrosis lungs. Infect Immun 81:2697–2704. https://doi.org/10.1128/IAI.00418-13.
53. O'Brien S, Williams D, Fothergill JL, Paterson S, Winstanley C, Brockhurst MA. 2017. High virulence subpopulations in *Pseudomonas aeruginosa* long-term cystic fibrosis airway infections. BMC Microbiol 17:30. https://doi.org/10.1186/s12866-017-0941-6.
54. Baishya J, Wakeman CA. 2019. Selective pressures during chronic infection drive microbial competition and cooperation. NPJ Biofilms Microbiomes 5:16. https://doi.org/10.1038/s41522-019-0089-2.
55. Mendonca CM, Yoshitake S, Wei H, Werner A, Sasnow SS, Thannhauser TW, Aristilde L. 2020. Hierarchical routing in carbon metabolism favors iron-scavenging strategy in iron-deficient soil *Pseudomonas* species. Proc Natl Acad Sci U S A 117:32358–32369. https://doi.org/10.1073/pnas.2016380117.
56. Raneri M, Pinatel E, Peano C, Rampioni G, Leoni L, Bianconi I, Jousson O, Dalmasio C, Ferrante P, Briani F. 2018. *Pseudomonas aeruginosa* mutants defective in glucose uptake have pleiotropic phenotype and altered virulence in non-mammal infection models. Sci Rep 8:16912. https://doi.org/10.1038/s41598-018-35087-y.
57. Wijesinghe G, Dilhari A, Gayani B, Kottegoda N, Samaranayake L, Weerasekera M. 2019. Influence of laboratory culture media on *in vitro* growth, adhesion, and biofilm formation of *Pseudomonas aeruginosa* and *Staphylococcus aureus*. Med Princ Pract 28:28–35. https://doi.org/10.1159/000494757.
58. Kannan A, Gautam P. 2015. A quantitative study on the formation of *Pseudomonas aeruginosa* biofilm. SpringerPlus 4:379–373. https://doi.org/10.1186/s40064-015-1029-0.
59. Gloag ES, Fabbri S, Wozniak DJ, Stoodley P. 2020. Biofilm mechanics: implications in infection and survival. Biofilm 2:100017. https://doi.org/10.1016/j.bioflm.2019.100017.
60. Kirienko DR, Revtovich AV, Kirienko NV. 2016. A high-content, phenotypic screen identifies fluorouridine as an inhibitor of pyoverdine biosynthesis and *Pseudomonas aeruginosa* virulence. mSphere 1:e00217-16.
61. Imperi F, Massai F, Facchini M, Frangipani E, Visaggio D, Leoni L, Bragonzi A, Visca P. 2013. Repurposing the antimycotic drug flucytosine for suppression of *Pseudomonas aeruginosa* pathogenicity. Proc Natl Acad Sci U S A 110:7458–7463. https://doi.org/10.1073/pnas.1222706110.
62. Kang D, Revtovich AV, Chen Q, Shah KN, Cannon CL, Kirienko NV. 2019. Pyoverdine-dependent virulence of *Pseudomonas aeruginosa* isolates from cystic fibrosis patients. Front Microbiol 10:2048. https://doi.org/10.3389/fmicb.2019.02048.
63. Merritt JH, Kadouri DE, O'Toole GA. 2005. Growing and analyzing static biofilms: current protocols in microbiology. Curr Protoc Microbiol Chapter 1:Unit 1B.1. https://doi.org/10.1002/9780471729259.mc01b01s00.
64. Irani VR, Rowe JJ. 1997. Enhancement of transformation in *Pseudomonas aeruginosa* PAO1 by Mg^{2+} and heat. Biotechniques 22:54–56. https://doi.org/10.2144/97221bm09.
65. Walters MC, Roe F, Bugnicourt A, Franklin MJ, Stewart PS. 2003. Contributions of antibiotic penetration, oxygen limitation, and low metabolic activity to tolerance of *Pseudomonas aeruginosa* biofilms to ciprofloxacin and tobramycin. Antimicrob Agents Chemother 47:317–323. https://doi.org/10.1128/AAC.47.1.317-323.2003.
66. Kroken AR, Chen CK, Evans DJ, Yahr TL, Fleiszig SM. 2018. The impact of ExoS on *Pseudomonas aeruginosa* internalization by epithelial cells is independent of *fleQ* and correlates with bistability of type three secretion system gene expression. mBio 9:e00668-18. https://doi.org/10.1128/mBio.00668-18.
67. Schmittgen TD, Livak KJ. 2008. Analyzing real-time PCR data by the comparative C T method. Nat Protoc 3:1101–1108. https://doi.org/10.1038/nprot.2008.73.

68. Edgar RC. 2004. MUSCLE: multiple sequence alignment with high accuracy and high throughput. Nucleic Acids Res 32:1792–1797. https://doi.org/10.1093/nar/gkh340.
69. Arkin AP, Cottingham RW, Henry CS, Harris NL, Stevens RL, Maslov S, Dehal P, Ware D, Perez F, Canon S, Sneddon MW, Henderson ML, Riehl WJ, Murphy-Olson D, Chan SY, Kamimura RT, Kumari S, Drake MM, Brettin TS, Glass EM, Chivian D, Gunter D, Weston DJ, Allen BH, et al. 2018. KBase: the United States department of energy systems biology knowledgebase. Nat Biotechnol 36:566–569. https://doi.org/10.1038/nbt.4163.
70. Price MN, Dehal PS, Arkin AP. 2010. FastTree 2: approximately maximum-likelihood trees for large alignments. PLoS One 5:e9490. https://doi.org/10.1371/journal.pone.0009490.
71. Aziz RK, Bartels D, Best AA, DeJongh M, Disz T, Edwards RA, Formsma K, Gerdes S, Glass EM, Kubal M, Meyer F, Olsen GJ, Olson R, Osterman AL, Overbeek RA, McNeil LK, Paarmann D, Paczian T, Parrello B, Pusch GD, Reich C, Stevens R, Vassieva O, Vonstein V, Wilke A, Zagnitko O. 2008. The RAST Server: rapid annotations using subsystems technology. BMC Genomics 9:75–15. https://doi.org/10.1186/1471-2164-9-75.
72. Smith R, Tan C, Srimani JK, Pai A, Riccione KA, Song H, You L. 2014. Programmed Allee effect in bacteria causes a tradeoff between population spread and survival. Proc Natl Acad Sci U S A 111:1969–1974. https://doi.org/10.1073/pnas.1315954111.
73. Wilson C, Lopatkin A, Craddock T, Eldakar O, Driscoll W, Lopez J, Smith R. 2017. Cooperation and competition shape ecological resistance during periodic spatial disturbance of engineered bacteria. Sci Rep 7:440. https://doi.org/10.1038/s41598-017-00588-9.
74. Jin Z, Li J, Ni L, Zhang R, Xia A, Jin F. 2018. Conditional privatization of a public siderophore enables *Pseudomonas aeruginosa* to resist cheater invasion. Nat Commun 9:1383. https://doi.org/10.1038/s41467-018-03791-y.
75. Kaplan JB. 2010. Biofilm dispersal: mechanisms, clinical implications, and potential therapeutic uses. J Dent Res 89:205–218. https://doi.org/10.1177/0022034509359403.
76. Nadal-Jimenez P, Koch G, Reis CR, Muntendam R, Raj H, Jeronimus-Stratingh CM, Cool RH, Quax WJ. 2014. PvdP is a tyrosinase that drives maturation of the pyoverdine chromophore in *Pseudomonas aeruginosa*. J Bacteriol 196:2681–2690. https://doi.org/10.1128/JB.01376-13.
77. Wibowo JP, Batista FA, van Oosterwijk N, Groves MR, Dekker FJ, Quax WJ. 2020. A novel mechanism of inhibition by phenylthiourea on PvdP, a tyrosinase synthesizing pyoverdine of *Pseudomonas aeruginosa*. Int J Biol Macromol 146:212–221. https://doi.org/10.1016/j.ijbiomac.2019.12.252.
78. Bartell JA, Blazier AS, Yen P, Thøgersen JC, Jelsbak L, Goldberg JB, Papin JA. 2017. Reconstruction of the metabolic network of *Pseudomonas aeruginosa* to interrogate virulence factor synthesis. Nat Commun 8:14631. https://doi.org/10.1038/ncomms14631.
79. Goss CH, Kaneko Y, Khuu L, Anderson GD, Ravishankar S, Aitken ML, Lechtzin N, Zhou G, Czyz DM, McLean K, Olakanmi O, Shuman HA, Teresi M, Wilhelm E, Caldwell E, Salipante SJ, Hornick DB, Siehnel RJ, Becker L, Britigan BE, Singh PK. 2018. Gallium disrupts bacterial iron metabolism and has therapeutic effects in mice and humans with lung infections. Sci Transl Med 10:eaat7520. https://doi.org/10.1126/scitranslmed.aat7520.
80. Yang L, Haagensen JAJ, Jelsbak L, Johansen HK, Sternberg C, Høiby N, Molin S. 2008. In situ growth rates and biofilm development of *Pseudomonas aeruginosa* populations in chronic lung infections. J Bacteriol 190:2767–2776. https://doi.org/10.1128/JB.01581-07.
81. Hagen SJ. 2014. The physical basis of bacterial quorum communication. Springer, New York, NY.
82. Song H, Payne S, Gray M, You L. 2009. Spatiotemporal modulation of biodiversity in a synthetic chemical-mediated ecosystem. Nat Chem Biol 5:929–935. https://doi.org/10.1038/nchembio.244.
83. Mah T-FC, O'Toole GA. 2001. Mechanisms of biofilm resistance to antimicrobial agents. Trends Microbiol 9:34–39. https://doi.org/10.1016/S0966-842X(00)01913-2.
84. Park AJ, Murphy K, Krieger JR, Brewer D, Taylor P, Habash M, Khursigara CM. 2014. A temporal examination of the planktonic and biofilm proteome of whole cell *Pseudomonas aeruginosa* PAO1 using quantitative mass spectrometry. Mol Cell Proteomics 13:1095–1105. https://doi.org/10.1074/mcp.M113.033985.
85. Kang D, Kirienko NV. 2017. High-throughput genetic screen reveals that early attachment and biofilm formation are necessary for full pyoverdine production by *Pseudomonas aeruginosa*. Front Microbiol 8:1707. https://doi.org/10.3389/fmicb.2017.01707.
86. Jin Z, Li J, Ni L, Zhang R, Xia A, Jin F. 2018. Conditional privatization of a public siderophore enables *Pseudomonas aeruginosa* to resist cheater invasion. Nat Commun 9:1383. https://doi.org/10.1038/s41467-018-03791-y.
87. Imperi F, Tiburzi F, Visca P. 2009. Molecular basis of pyoverdine siderophore recycling in *Pseudomonas aeruginosa*. Proc Natl Acad Sci U S A 106:20440–20445. https://doi.org/10.1073/pnas.0908760106.
88. Sauer K, Cullen MC, Rickard AH, Zeef LAH, Davies DG, Gilbert P. 2004. Characterization of nutrient-induced dispersion in *Pseudomonas aeruginosa* PAO1 biofilm. J Bacteriol 186:7312–7326. https://doi.org/10.1128/JB.186.21.7312-7326.2004.
89. Morgan R, Kohn S, Hwang S-H, Hassett DJ, Sauer K. 2006. BdlA, a chemotaxis regulator essential for biofilm dispersion in *Pseudomonas aeruginosa*. J Bacteriol 188:7335–7343. https://doi.org/10.1128/JB.00599-06.
90. Gjermansen M, Ragas P, Sternberg C, Molin S, Tolker-Nielsen T. 2005. Characterization of starvation-induced dispersion in *Pseudomonas putida* biofilms. Environ Microbiol 7:894–904. https://doi.org/10.1111/j.1462-2920.2005.00775.x.
91. Musk DJ, Banko DA, Hergenrother PJ. 2005. Iron salts perturb biofilm formation and disrupt existing biofilms of *Pseudomonas aeruginosa*. Chem Biol 12:789–796. https://doi.org/10.1016/j.chembiol.2005.05.007.